Contribution from the Kenan Laboratories of Chemistry,
The University of North Carolina, Chapel Hill, North Carolina 27514

Kinetic Applications of Chemically Modified Electrodes. Oxidation, Reduction, and Linkage Isomerization of a Nitro Complex of Ruthenium Attached to a Silanized Platinum Electrode

H. D. ABRUÑA, J. L. WALSH, T. J. MEYER, and ROYCE W. MURRAY*

Received May 30, 1980

The complex $[(bpy)_2Ru(i\text{-nic})NO_2]^+$ (*i*-nic = isonicotinic acid) can be attached to alkylaminesilanized platinum oxide electrode surfaces by amide coupling. Electrochemical oxidation of the complex initiates reactions qualitatively similar to those observed for the unattached, oxidized complex, but with substantial alterations in rates. The reactions can be followed electrochemically by observing the cyclic voltammetric surface waves of the electrodes at room and low (−78 °C) temperature. Oxidation of the attached complex is rapidly followed by a reversible linkage isomerization to the O-bound (nitrito) complex. On a much longer time scale, the complex reacts, irreversibly, by two competing reaction paths, to yield to mixture of nitrosyl and nitrato complexes where the latter predominates.

We recently described[1] the covalent surface attachment of monomolecular layers of 2,2′-bipyridyl (bpy) complexes of ruthenium to Pt electrodes using the reactions

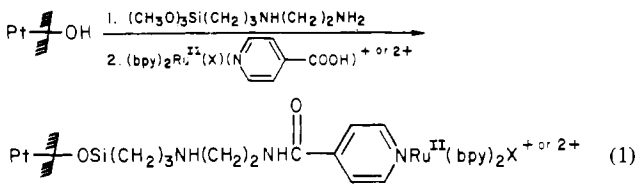

(1)

I

where X was isonicotinic acid or chloride. In CH_3CN containing 0.1 M Et_4NClO_4 electrolyte, these surfaces exhibited stable electrochemical current–potential waves corresponding to cycling of I between Ru(II) and Ru(III) oxidation states. Our initial success encouraged us to explore the similar attachment of the Ru(II) complex where X ≡ NO_2^-, i.e., the attachment of $[(bpy)_2Ru^{II}(i\text{-nic})NO_2]^+$ (II) (*i*-nic = isonicotinic acid (4-pyridinecarboxylic acid)). The nitro complex was of interest since solution studies[2] have shown that in the Ru(III) state, $[(bpy)_2Ru^{III}(py)NO_2]^{2+}$ disproportionates to $[(bpy)_2Ru^{III}(py)ONO_2]^{2+}$ and $[(bpy)_2Ru^{II}(py)NO]^{3+}$ and, in an electrochemically driven cycle, catalytically oxidizes triphenylphosphine to triphenylphosphine oxide.[3] An examination of the chemical and electrochemical properties of I where X ≡ NO_2^- demonstrated that the immobilized nitro complex undergoes the same general reactions as its solution analogue, but at significantly different rates.[4] Particularly interesting, in light of the presumably rather concentrated environment in the monomolecular layer, was the much slower reaction rate observed for disproportionation of the immobilized $Ru^{III}NO_2$ complex. A more detailed kinetic and mechanistic study of the disproportionation reaction for the immobilized $Ru^{III}NO_2$ complex was the object of experiments reported here.

During our study, five aspects of modified electrode behavior were instrumental in unraveling the complex and rapid $Ru^{III}NO_2$ disproportionation reaction mechanism. One was that the usual simulation of coupling of solution diffusion kinetics with chemical reaction kinetics and mechanism was unnecessary. A second was the retardation of the overall disproportionation rate for immobilized $Ru^{III}NO_2$ complex as mentioned above. The third was the simplicity of carrying out low-temperature electrochemical experiments (−78 °C, in butyronitrile) with the modified electrodes, without complications from reactant solubility or need to account for alterations in diffusion rates associated with a homogeneous reaction.[5] The low-temperature electrochemistry both allowed the disproportionation reaction to be literally "frozen" and facilitated detection and study of a critical intermediate in the reaction.

The fourth advantage was that it was possible to employ much higher cyclic voltammetric potential sweep rates (v) with the modified electrodes than is conventionally feasible with dissolved reactants. Peak currents for dissolved reactants vary with $v^{1/2}$ (v = potential scan rate) whereas electrode double-layer charging currents are proportional to v, so it is typical that in the 10–50 V/s range, signal/background for the desired Faradaic wave degrades considerably. A monolayer of an immobilized, reversible redox couple, on the other hand, behaves as a pseudocapacitance so that its peak current shows the same potential sweep rate dependency as the superimposed double-layer charging background current.[6] Sweep rates of 200 V/s can as a result be used with relative ease without signal/background degradation. Although self-evident, this kinetic advantage, inherent in the study of immobilized redox systems, has escaped prior mention.

The fifth advantage arose from the *isopotential points* which appeared in the cyclic voltammetry of I (where X ≡ NO_2^-) during its chemical transformations to products. Isopotential points are the electrochemical equivalent of spectrophotometric isosbestic points, and for surface species have the same mechanistic usefulness, connecting a specific reactant and product. They do not appear in the electrochemistry of dissolved reactants because of the intervention of diffusion kinetics. According to Untereker and Bruckenstein,[7] an isopotential point in a changing array of surface waves denotes a simple correspondence between a reactant wave and a product wave at a constant combined surface coverage of the two.

The advantages summarized above are distinctly notable for the study of reaction mechanisms. Their successful application to the elucidation of the $Ru^{III}NO_2$ disproportionation

(1) Abruña, H. D.; Meyer, T. J.; Murray, R. W. *Inorg. Chem.* **1979**, *18*, 3233.
(2) Keene, F. R.; Salmon, D. J.; Walsh, J. L.; Abruña, H. D.; Meyer, T. J. *Inorg. Chem.* **1980**, *19*, 1896.
(3) Keene, F. R.; Salmon, D. J.; Meyer, T. J. *J. Am. Chem. Soc.* **1977**, *99*, 4821.
(4) Abruña, H. D.; Walsh, J. L.; Meyer, T. J.; Murray, R. W. *J. Am. Chem. Soc.* **1980**, *102*, 3272.
(5) Van Duyne, R. P.; Reilley, C. N. *Anal. Chem.* **1972**, *44*, 142.
(6) Lane, R. F.; Hubbard, A. T. *J. Phys. Chem.* **1973**, *77*, 1401.
(7) Untereker, D. F.; Bruckenstein, S. *Anal. Chem.* **1972**, *44*, 1009.

0020-1669/81/1320-1481$01.25/0

mechanism suggests that in appropriate cases, attachment to an electrode surface can be a powerful mechanistic tool.

Experimental Section

Electrode Pretreatment. The surfaces of mirror polished (1-μm diamond paste) Pt-disk electrodes were oxidized by twice dipping in concentrated nitric acid (5 min each time) followed by a distilled water wash. The thoroughly washed electrodes were vacuum dried at 50 °C for 20 min.

Electrode Silanization. The superficially oxidized Pt electrodes, in serum-capped vials flushed with a positive pressure of dry N_2, were washed with dry toluene for ca. 5 min and then allowed to react with an anhydrous, 15% toluene solution of (3-((2-aminoethyl)amino)-propyl)trimethoxysilane (enpt silane) for 5 min at room temperature. The silanized electrodes were washed six times with dry toluene under N_2 and twice with dichloromethane.

Attachment of the Ruthenium Complex. The silanized electrodes were allowed to react in the dark with ca. 1–3 mM solutions of $[(bpy)_2Ru^{II}(i\text{-nic})NO_2]^+$ (II) in methylene chloride in the presence of excess *N,N'*-dicyclohexylcarbodiimide for 20–24 h. After reaction, the modified electrodes were washed with acetone (2×) and dichloromethane (4×) and stored in a closed vial.

Synthesis. $[Ru(bpy)_2(py)NO_2](PF_6)$ **(III)** was prepared as previously described.[2]

$[Ru(bpy)_2(i\text{-nic})NO_2](PF_6)$ **(II).** $Ru(bpy)_2Cl_2\cdot 2H_2O$ was allowed to react with a 37% molar excess of methyl isonicotinate by heating in 50/50 v/v $EtOH/H_2O$ solution at reflux for 45 min. A 22% molar excess of $NaNO_2$ was added to the cooled reaction mixture which has then heated further at reflux for 2.5 h. After cooling, the reaction mixture was reduced to half the initial volume and refrigerated overnight. The cooled solution was filtered, to remove a red precipitate, presumably $Ru(bpy)_2(NO_2)_2$, and the desired complex was precipitated from the filtrate by addition of 2 mL of saturated aqueous NH_4PF_6. The precipitate was collected and washed with H_2O, CH_3OH, and diethyl ether. The solid was partially dissolved in methylene chloride, and the undissolved material was collected and washed as before. This process was repeated on the undissolved material that was collected. The remaining solid was dissolved in a minimum volume of acetonitrile, reprecipitated with ether, collected, and washed with ether. It was then suspended in ca. 15 mL of H_2O and enough acetonitrile added to dissolve the complex. A 0.5-mL portion of 1 M NaOH was added to this solution which was allowed to stir at ca. 50 °C for 45 min, after which the complex was precipitated by the addition of HPF_6, collected, and washed with ether. The solid was dissolved in acetonitrile containing 0.5 mL of lutidine and 0.25 mL of water and stirred at room temperature for 30 min. The solid was reprecipitated by the addition of ether, collected, washed with ether, and dried. Characterizations by cyclic voltammetry and spectroscopy ($E_{p,a}$ = +1.06 V vs. SSCE for $Ru^{II}NO_2$ oxidation, visible λ_{max} = 432 nm, infrared $\nu(NO_2)$ at 1290, 1340 cm^{-1}) were consistent with the proposed formulation of II as a pyridine carboxylic acid, nitro complex. Anal. Calcd: C, 42.92; H, 2.91; N, 11.55. Found: C, 42.09; H, 2.21; N, 10.93.

Reagents. Silane. (3-((2-Aminoethyl)amino)propyl)trimethoxysilane (enpt silane) (PCR or Petrarch) was vacuum distilled twice and stored in a desiccator.

Solvents. Spectrograde acetonitrile (MCB) and reagent grade dichloromethane were dried over 4-Å molecular sieves. Reagent grade toluene was dried over metallic sodium. Butyronitrile (Eastman), BuCN, was passed through a column of activated alumina and then distilled under N_2 from $KMnO_4$ (11.5 g/L) and Na_2CO_3 (7.7 g/L), redistilled from CaH_2, and stored over 4-Å molecular sieves under N_2. Other solvents were of at least reagent grade quality and used as received.

Chemicals. Tetraethylammonium perchlorate (Eastman), Et_4NClO_4, was recrystallized three times from water and dried in vacuo at 100 °C for 72 h. Tetra-*n*-butylammonium perchlorate (G. F. Smith), Bu_4NClO_4, was vacuum dried at 60 °C for 48 h. Other chemicals were used as received.

Instrumentation and Procedure. Visible and UV spectra were obtained on a Model 210 Bausch and Lomb spectrophotometer; IR spectra, on a Model 4250 Beckman spectrophotometer. A conventionally designed operational amplifier-based three-electrode potentiostat with positive feedback *iR* compensation or a Wenking Model 611R potentiostat were used in electrochemical experiments. Triangular wave forms were supplied by a locally designed[8] signal generator or a Princeton Applied Research Model 175 Universal Programmer. Cyclic voltammograms were recorded using a Hewlett-Packard Model 7004B X-Y recorder or a Model 564B Tektronix storage oscilloscope. A Faraday cage was used to minimize noise. For the experiments conducted at low temperature or fast potential sweep rates, resistance compensation was employed.

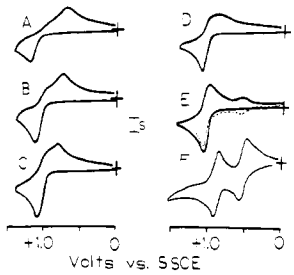

Figure 1. Cyclic voltammetry of $[(bpy)_2Ru(py)NO_2]^+$ in 0.1 M Et_4NClO_4/CH_3CN. Curves A–E, scan rate dependency: curve A, 50 V/s (S = 200 μA); curve B, 20 V/s (S = 100 μA); curve C, 5 V/s (S = 50 μA); curve D, 3 V/s (S = 50 μA); curve E, 0.5 V/s (S = 20 μA) (two scans). Curve F: same solution after exhaustive electrolysis at 1.2 V; v = 0.2 V/s (S = 5 μA).

The supporting electrolyte/solvent systems employed were 0.1 M Et_4NClO_4/CH_3CN for room temperatre measurements and 0.1 M $Bu_4NClO_4/BuCN$ at low temperatures. Low-temperature experiments were conducted in a cell immersed in a 2-propanol/dry ice bath (−78 °C). The reference electrode was held at room temperature and connected to the low-temperature cell with a 0.1 M $Bu_4NClO_4/BuCN$ bridge. All electrochemical experiments were conducted in a cell of conventional design with a Luggin probe. The reference electrode was a sodium chloride saturated calomel electrode (SSCE).

Results

CH_3CN Solutions of $[(bpy)_2Ru^{II}(py)NO_2]^+$ (III). Electrooxidation of the nitro complex III to Ru(III) is followed by a series of fast reactions leading to net disproportionation of the nitro ligand to yield ruthenium nitrato and nitrosyl complexes:[2]

$$2[(bpy)_2Ru^{II}(py)NO_2]^+ \xrightarrow{-3e^-} [(bpy)_2Ru^{III}(py)ONO_2]^{2+} + [(bpy)_2Ru^{II}(py)NO]^{3+} \quad (2)$$

This is illustrated by cyclic voltammetry (Figure 1, curve E), in which the anodic wave at $E_{p,a}$ = +1.06 V vs. SSCE for the $Ru^{II}NO_2/Ru^{III}NO_2$ reaction is followed by a relatively broad, cathodic wave at $E_{p,c}$ = +0.91 V and another, smaller cathodic wave at $E_{p,c}$ = +0.48 V vs. SSCE. A subsequent oxidative sweep shows that the latter wave is associated with the reversible nitrosyl couple $[(bpy)_2Ru(py)NO]^{3+/2+}$ and that the former broad cathodic wave consists of overlapping waves for the nitrato couple $[(bpy)_2Ru(py)ONO_2]^{2+/+}$ and for a small amount of unreacted nitro complex $[(bpy)_2Ru(py)NO_2]^{2+/+}$. This interpretation is supported by exhaustive electrolysis at 1.2 V vs. SSCE in acetonitrile of a solution of III which gives the cyclic voltammogram in Figure 1, curve F. The product waves at $E_{soln}^{o'}$ = +0.91 and +0.49 V vs. SSCE represent the nitrato and nitrosyl couples, respectively, obtained in a 1/1 ratio.

Further information is obtained at faster sweep rates as shown in Figure 1. As the sweep rate increases (curves E → A), the cathodic wave for the nitrosyl product disappears (compare curves E and D) and a new cathodic wave with $E_{p,c}$ = 0.72 V vs. SSCE appears and grows until, at the fastest sweep rate (50 V/s, curve A), it is the dominant cathodic product. The definition of the waves at the fast potential sweep is marginal, and it becomes difficult to say whether the

(8) Woodward, W. S.; Rocklin, R. D.; Murray, R. W. *Chem., Biomed. Environ. Instrum.* **1979**, *9*, 95.

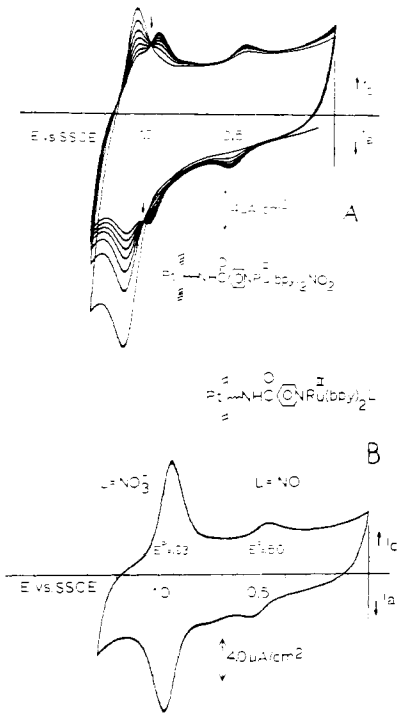

Figure 2. Room-temperature cyclic voltammetry of Pt/PtO/Si-$(CH_2)_3NH(CH_2)_2NH(i\text{-nic})[Ru(bpy)_2NO_2]^+$ in 0.1 M Et_4NClO_4/CH_3CN at 0.2 V/s (current sensitivity 4 $\mu A/cm^2$): A, curves for first seven cyclical potential scans (arrows denote isopotential points); B, curve after 40 scans and complete reaction.

cathodic wave at $E_{p,c} \approx 0.72$ V represents unreacted $[(bpy)_2Ru(py)NO_2]^{2+}$ or nitrato complex. If the solution voltammetry is conducted at −78 °C, a similar pattern is observed but in this case a cathodic counterpart of the wave at $E_{p,c} = +0.72$ V could be observed so that a formal potential $E_{soln}^{o'} = +0.80$ V vs. SSCE could be estimated. This latter species is inferred to be an intermediate in the disproportionation process.

Electrodes with Attached $[(bpy)_2Ru^{II}(i\text{-nic})NO_2]^+$. We will designate electrodes which have been modified to bear the surface structure

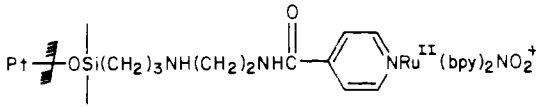

as $Pt/\sim Ru^{II}NO_2$. Room-temperature cyclic voltammetry of a thus modified electrode in 0.1 M Et_4NClO_4/CH_3CN as illustrated in Figure 2 was conducted at the same potential scan rate (0.2 V/s) as the solution voltammogram in Figure 1E. A reduction counterpart of the oxidation wave for $Pt/\sim Ru^{II}NO_2$ is clearly evident on the reverse sweep of the initial potential cycle, and little disproportionation has occurred. As we reported in a preliminary account,[4] this result contrasts sharply with the homogeneous data (Figure 1E) and indicates that the disproportionation reaction occurs more slowly for the immobilized nitro complex. On the second and following cyclical potential scans, the waves for the $Pt/\sim RuNO_2$ couple ($E_{surf}^{o'} = +1.04$ V vs. SSCE) gradually diminish, and waves at potentials appropriate for the nitrato ($E_{surf}^{o'} = +0.93$ V) and nitrosyl ($E_{surf}^{o'} = +0.50$ V vs. SSCE) complexes grow. It is evident in Figure 2A that, due to the symmetrical character of electrochemical surface waves, the nitro and nitrato waves are much better resolved from one another than in the solution voltammetry (i.e., Figure 1E). Furthermore, a well-defined isopotential point (Figure 2A, arrows) occurs between these two waves, indicating that the nitro wave decay and nitrato wave growth are closely related processes.

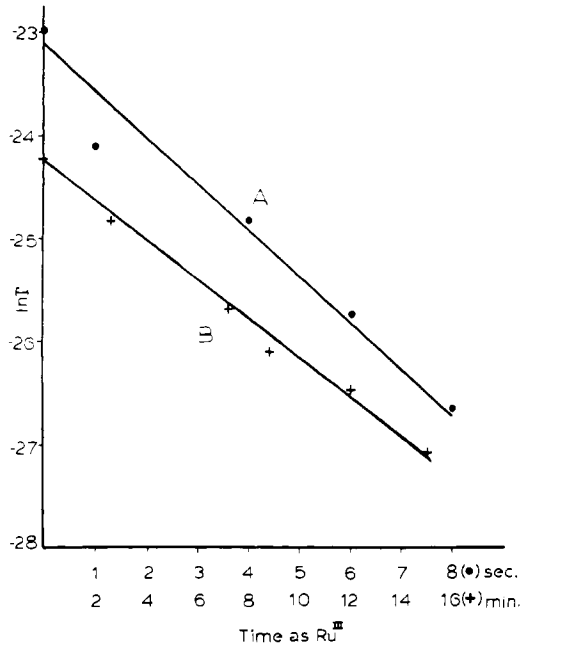

Figure 3. First-order decay plots for $Pt/PtO/Si(CH_2)_3NH(CH_2)_2NH(i\text{-nic})[Ru(bpy)_2NO_2]^+$: A (●), decay at room temperature, $k = 0.5$ s^{-1}; B (+), decay at low temperature (*i*-PrOH/dry ice, −78 °C), $k = 3 \times 10^{-3}$ s^{-1}.

If cyclical potential scanning is continued, a constant pattern of product waves is eventually obtained and the $Pt/\sim RuNO_2$ wave completely disappears. The combined charge under the two product waves in Figure 2B corresponds to a total ruthenium complex coverage of $\Gamma = 0.44 \times 10^{-10}$ mol/cm.^{2} as compared to $\Gamma_{RuNO_2} = 0.50 \times 10^{-10}$ mol/cm.^{2} for the initial $Pt/\sim Ru^{II}NO_2$ reactant coverage estimated from the initial anodic wave in Figure 2A. These coverages are typical and are in the loosely compacted monomolecular range for complexes of this size (average radius 6–7 Å).

Figure 2B is further notable on two accounts. First, the quantity of nitrato ($Pt/\sim RuONO_2$) product exceeds that of nitrosyl ($Pt/\sim RuNO$) product. The ratio of these two product complexes varies from electrode to electrode but most typically was $\gg 1/1$ as shown, an observation which must be accounted for in developing a complete reactivity picture for $Pt/\sim RuNO_2$. The second notable feature is that ΔE_p, the potential difference between the anodic and cathodic peak currents, for the nitrosyl surface waves $Pt/\sim RuNO$, 80–100 mV, is much larger than ΔE_p for the nitrato surface waves, $Pt/\sim RuONO_2$, 10–30 mV. In solution (Figure 1F) the peak potential separations for nitrato and nitrosyl complexes are similar and near their reversible values (60 and 60 mV, respectively). Peak separation (ΔE_p) for reversible (limit of fast electron transfer) surface waves is ideally zero.[6] Evidently, electron transfer to and from the bound nitrosyl complex to the electrode has a kinetic inhibition associated with it.

The rate of the reaction of $Pt/\sim Ru^{III}NO_2$ occurring in Figure 2A was evaluated by measuring the charge under its oxidative wave (i.e., its coverage Γ_{RuNO_2}) as a function of time. Since the instability of the surface redox couple is associated only with the $Pt/\sim Ru^{III}NO_2$ state, the time axis in the analysis was taken as the cumulative time that a potential more positive than $E_{surf}^{o'}$ for the $Pt/\sim Ru^{III/II}NO_2$ couple was applied. A plot of $\ln[\Gamma_{RuNO_2}]$ vs. time (first-order rate law) is reasonably linear (Figure 3, curve A), whereas one of $1/\Gamma_{RuNO_2}$ vs. time (second-order rate law) is not. The kinetic data show that the reaction of the nitro complex is first order in $Pt/\sim Ru^{III}NO_2$.

$$d\Gamma_{RuNO_2}/dt = -k\Gamma_{Ru^{III}NO_2} \quad (3)$$

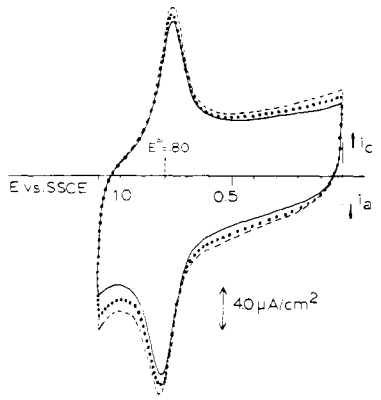

Figure 4. Variable-temperature electrochemistry for Pt/PtO/Si-$(CH_2)_3NH(CH_2)_2NH(i\text{-nic})[Ru(bpy)_2Cl]^+$ at 0.2 V/s in 0.1 M *n*-Bu_4ClO_4/BuCN (current sensitivity 4 μA/cm²): (—) T = −78 °C; (···) T = −48 °C; (- - -) T = +26 °C.

The slope of curve A in Figure 3 yields a rate constant k = 0.5 s^{-1} for the process observed.[9] However, since the results of Figures 1 and 2B suggest that the overall mechanism is complex, the meaning of the rate law observed in the decay kinetics is not clear, and low-temperature experiments were initiated at this point.

Low-temperature experiments have not previously been employed for electrodes modified with monolayers of electroactive sites, including electrodes based on organosilane attachments. Accordingly, we first studied, as a model compound, the complex $[(bpy)_2Ru(i\text{-nic})Cl]^+$ attached as in reaction 1, since we knew that the Pt/~~$Ru^{III/II}Cl$ reaction for this couple was reversible[1] and fairly stable at room temperature. As seen in Figure 4, the surface wave for the chloro complex in butyronitrile/0.1 M Bu_4NClO_4 remains essentially unchanged in terms of ΔE_p, Γ, and wave shape over a 100 °C temperature range. On the voltammetric time scale, electron transfer to and from the attached couple remains facile over the entire temperature range. The electrochemical result is consistent with the low energy of activation observed for the homogeneous $Ru(bpy)_2(py)Cl^{2+/+}$ self-exchange reaction in acetonitrile[10], but it should be noted that the vibrational barrier to electron transfer on the surface could include additional vibrational orders associated with organosilane chain reorientations or "flopping" motions[11] required to bring the redox site toward the electrode surface. Presumably these vibrational barriers to electron transfer for the Pt/~~$RuNO_2$ couple are also small.

Figure 5 shows that the reactivity of Pt/~~$Ru^{III}NO_2$ is substantially retarded by a decrease in temperature to −78 °C. The electrode potential can be repeatedly scanned with only small changes in the cyclic voltammogram, curve A. At longer cumulative scanning times the decay reaction does slowly occur, nitrato and nitrosyl product waves are again obtained

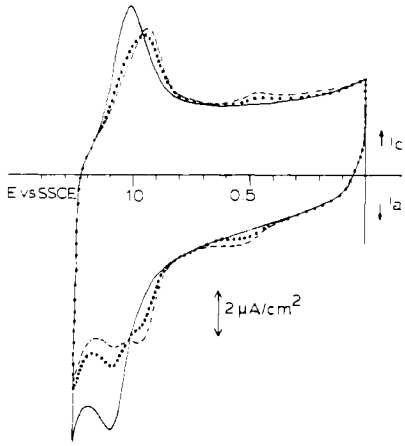

Figure 5. Electrochemistry of Pt/PtO/$Si(CH_2)_3NH(CH_2)_2NH(i\text{-nic})[Ru(bpy)_2NO_2]^+$ at −78 °C in 0.1 M *n*-Bu_4ClO_4/BuCN at a sweep rate of 0.2 V/s (current sensitivity 2 μA/cm²), scans being taken after (curve A —) 30 s, (curve B ···) 16 min, and (curve C - - -) 29 min of continuous scanning.

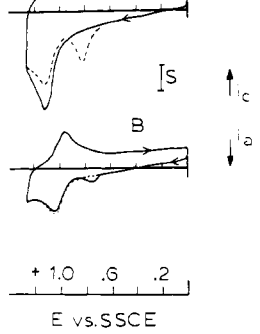

Figure 6. Electrochemistry of Pt/PtO/$Si(CH_2)_3NH(CH_2)_2NH(i\text{-nic})[Ru(bpy)_2NO_2]^+$ at −78 °C in 0.1 M Bu_4ClO_4/BuCN. Curve A: solid line is first scan, 3 V/s; dashed line is second scan, 3 V/s, immediately following the first scan or delayed for t < 10 min; S = 24 μA/cm². Curve B: solid line is scan at 0.2 V/s taken after curve A (dashed-line scan); dashed line is second scan at 0.2 V/s; S = 4.9 μA/cm².

(curve C, Figure 5), and the nitrato/nitrosyl product ratio is both >1/1 and larger than at room temperature. The low-temperature reaction again conforms to and supports (Figure 3B) a rate law, eq 3, which is first order in Pt/~~$Ru^{III}NO_2$. The value of k at −78 °C is 3×10^{-3} s^{-1} or a decrease of 160× as compared to the room-temperature result.

Low-temperature voltammetry at faster potential sweep rates proved particularly informative. As shown in Figure 6, curve A, for $v \geq 3$ V/s, an electrode for which no significant reaction to the nitrato and nitrosyl complexes has taken place exhibits almost no rereduction at $E_{p,c}$ = +1.02 V for Pt/~~$Ru^{III}NO_2$ but instead displays a cathodic wave at $E_{p,c}$ = +0.77 V vs. SSCE. On a second, immediately following, anodic potential scan, at ≥3 V/s, or on a scan deferred (at 0 V) for a few minutes (<10 min), an anodic counterpart (dashed curve, Figure 6A) of this new wave appears which shows it to be a reversible reaction with $E_{surf}^{\circ\prime}$ = +0.80 V vs. SSCE. A steady-state cyclic voltammogram at $v \geq 3$ V/s continues the pattern seen in Figure 6A, dashed curve, of an anodic wave for Pt/~~$Ru^{II}NO_2$ with little cathodic counterpart and a cathodic/anodic couple at +0.80 V in which the cathodic component appears to involve a greater amount of charge than the anodic. If, on the other hand, after an initial potential scan cycle at 3 V/s, further cycles are carried out at a *slower* scan

(9) It should be mentioned here that if, during the $Ru^{II}NO_2$ to $Ru^{III}NO_2$ oxidation, some disproportionation occurs to yield nitrato and nitrosyl products, the nitrosyl product will lose another electron in an "ECE" type process and thus will contribute to the wave at E_{pa} = 1.06 V. In the kinetic analysis we have assumed that the contribution of the nitrosyl product to the wave at E_{pa} = 1.06 V is small. This assumption is well justified in the experiments performed at low temperature or fast sweep rates (at room temperature) since very little nitrosyl product is formed. In the room-temperature measurements at slow sweep rates (0.2 V/s) the assumption is good after the first two cycles (since most of the nitrosyl product forms during these) but is approximate during the first two. However, even in the first two scans, the amount of nitrosyl product formed is small enough that it will not significantly affect the results.

(10) Callahan, R. W.; Keene, F. R.; Meyer, T. J.; Salmon, D. J. *J. Am. Chem. Soc.* **1977**, *99*, 1064.
(11) Moses, P. R.; Murray, R. W. *J. Am. Chem. Soc.* **1976**, *98*, 7435.

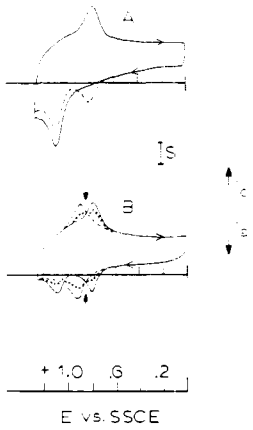

Figure 7. Room-temperature cyclic voltammetry of Pt/PtO/Si-$(CH_2)_3NH(CH_2)_2NH(i\text{-nic})[Ru(bpy)_2NO_2]^+$ in 0.1 M Et_4NClO_4/MeCN at 200 V/s with iR compensation; S = 3.65 $\mu A/cm^2$. Curve A: solid line, first scan; dashed line, second scan immediately following the first or delayed for $t < 10$ s. Curve B, electrode from curve A scanned continuously at 200 v/s and showing reaction of the ruthenium nitro complex (arrows denote isopotential points): (—) scan before appreciable reaction; (···) scan after partial reaction; (- - -) scan after nearly complete reaction.

rate, say 0.2 V/s, the wave at $E_{p,a}$ = +0.79 V is seen only on the *first* of these slower sweeps, Figure 6B, solid curve. Thereafter, the voltammogram (dashed curve) reverts to simply the Pt/$\sim$$Ru^{III/II}NO_2$ wave which is like that observed in Figure 5, curve A. This sequence of observations, in which the +0.80 V couple appears at fast scan rates and the Pt/$\sim$$Ru^{III}NO_2$ reduction wave reappears at slow scan rate, can be repeated many times on a single electrode, at low temperatures.

Phenomena similar to these can also be observed for Pt/$\sim$$RuNO_2$ electrodes at room temperature, if much faster potential sweep rates are employed. Figure 7A (solid curve) shows a voltammogram conducted at 200 V/s, whose appearance is very similar to that of Figure 6A and which has a very respectable wave definition even at this extreme scan rate. [For the anodic wave at $E_{p,a}$ = +0.82 V (Figure 7A, dashed curve) to be observed, the time elapsed between scans must be less than 30 s.] If the electrode is allowed to freely cycle at this rate, so that decay slowly occurs as it did in Figure 2, we see (Figure 7B) that the anodic Pt/$\sim$$Ru^{II}NO_2$ wave and the couple at +0.80 V decrease and are replaced by reversible waves at the potential of the nitrato and nitrosyl couples. The striking feature of the voltammogram in Figure 7B is that the isopotential point now occurs between the wave for nitrato complex and that of the couple at $E_{surf}^{\circ\prime}$ = +0.80 V. This behavior definitely establishes the species reacting at +0.80 V is the direct precursor of the immobilized nitrato complex and thus is an intermediate in the overall reaction.

Discussion

On the basis of the results presented above, the mechanism shown in Scheme I is proposed for the reaction of Pt/$\sim$$Ru^{III}NO_2$. This mechanism is consistent in qualitative details with the one proposed earlier for the related, homogeneous reaction[2] but differs in apparent elements of rate control and in the importance of the k_3 path.

Consider first the relationship of the scheme to voltammetric results acquired where little or no reaction producing the nitrosyl or nitrato complexes has yet occurred. At *fast* reverse (cathodic) potential scan rates (Figures 6A, 7A), the Pt/$\sim$$Ru^{III}NO_2$ resulting from oxidation of the original Pt/$\sim$$Ru^{II}NO_2$ has rapidly converted into an intermediate complex which becomes reduced at $E_{surf}^{\circ\prime}$ = +0.80 V vs. SSCE. Since the conversion at room temperature (k_1) is fast compared to

Scheme I

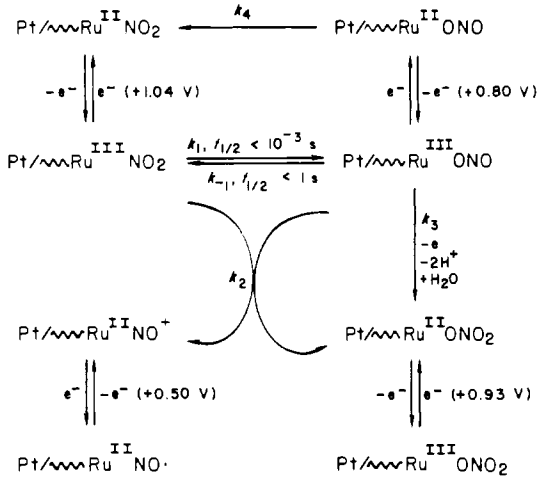

the time required (in the cathodic scan) to traverse the Pt/$\sim$$Ru^{III}NO_2$ potential region at 200 V/s, the $t_{1/2}$ for formation of the intermediate is estimated as $t_{1/2} < 10^{-3}$ s.

As indicated in the scheme, we propose that the rapidly formed intermediate is the O-bound (nitrito) linkage isomer Pt/$\sim$$Ru^{III}ONO$. Once reduced, the Pt/$\sim$$Ru^{II}ONO$ species reisomerizes back to the original Pt/$\sim$$Ru^{II}NO_2$ isomer, but the reaction is slow (k_4), requiring a few seconds at room temperature and up to 10 min (Figure 6A) at −78 °C. The linkage isomerization is in contrast rapidly reversible for the oxidized complexes. Pt/$\sim$$Ru^{III}ONO$ reisomerizes (k_{-1}) to Pt/$\sim$$Ru^{III}NO_2$ with $t_{1/2} < 1$ s at both room and low temperature as shown by voltammetry at *slow* potential scan rates (0.2 V/s; Figures 2A, 5, 6B). In these voltammograms, Pt/$\sim$$Ru^{III}ONO$ reisomerizes and becomes reduced as Pt/$\sim$$Ru^{III}NO_2$ because the reisomerization reaction k_{-1} occurs on a time scale short in comparison to the time required to scan to the Pt/$\sim$$Ru^{III}ONO$ wave at 0.2 V/s. The situation of starting a reverse potential scan (from +1.25 V) on an electrode now mostly in the Pt/$\sim$$Ru^{III}ONO$ state and observing the Pt/$\sim$$Ru^{III}NO_2$ wave at slow sweep rates but the Pt/$\sim$$Ru^{III}ONO$ wave at fast ones corresponds to the classical "CE" reaction mechanism of electrochemistry.[12] This is the first report of a CE mechanism in the electrochemistry of attached substances.

Consider now the process(es) leading to the final products of Pt/$\sim$$Ru^{II}NO_2$ oxidation, the nitrosyl and nitrato complexes. The appearance of the O-bound nitrato complex implies a change from N-bound to O-bound coordination at some reaction step following Pt/$\sim$$Ru^{II}NO_2$ oxidation, and the isomerization reaction (k_1) coveniently satisfies this requirement. A viable route to products would involve a bridged intermediate or activated complex from neighboring nitro and nitrito sites

$$\text{Pt/}\sim\text{RuNO}_2^{2+(\text{or }1+)} + \text{Pt/}\sim\text{Ru}^{III}\text{ONO}^{2+} \xrightarrow{k_2} [\text{Pt/}\sim\text{Ru–ONO–O–NO–Ru}\sim\text{/Pt}]^{4+(\text{or }3+)} \rightarrow \text{Pt/}\sim\text{Ru}^{III}\text{ONO}_2 + \text{Pt/}\sim\text{RuNO}^{3+(\text{or }2+)} \quad (4)$$

This is the k_2 pathway in the scheme, which would yield a 1/1 mixture of nitrosyl and nitrato complexes. When oxidized by a stoichiometric quantity of oxidant in homgeneous (acetonitrile) solution, $[(bpy)_2Ru(py)NO_2]^+$ also yields a 1/1 nitrato/nitrosyl product ratio[2], presumably by the same pathway.

(12) Brown, E. R.; Large, R. F. In "Physical Methods of Chemistry"; Weissberger, A., Rossiter, B. W., Eds.; Wiley: New York, 1971; Vol. I, Part 2A, p 423.

The experimental results of Figures 2B, 5, and 7B make clear that an additional pathway to the nitrato complex exists, since it typically is produced in greater quantity than the nitrosyl. This reaction likely occurs from the O-bound (nitrito) isomer Pt/~~Ru^{III}ONO as indicated in the scheme. A related reaction may exist in homogeneous solution, since if the starting complex $[(bpy)_2Ru(py)NO_2]^+$ is oxidized by an excess of $[Ru(bpy)_3]^{3+}$ in acetonitrile,[13] an excess of nitrato over nitrosyl product appears. In the attached case, the "excess" oxidant is the electrode. On the electrode surface, perhaps the (k_3) reaction involves platinum oxide surface states, possibly as

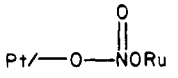

Such oxide states would be continually replenished, on a monomolecular basis, in the small anodic background currents which underlie the surface waves and which undoubtedly involve trace solvent water to some extent. Whatever the details of this reaction, it effectively completes with eq 4, at room and low temperature but more at the latter.

The isopotential points in Figures 2A and 7B provide further mechanistic insights. In a fast reverse (cathodic) potential scan at room temperature, the attached complex is reduced from the Pt/~~Ru^{III}ONO state (Figure 7A) as discussed above. As reaction to produce nitrato complex proceeds, the nitrato Pt/~~RuONO$_2$ wave grows, that for Pt/~~RuONO diminishes, and an isopotential point between the two waves shows that the loss in surface population of Pt/~~RuONO is nearly exactly balanced by the appearance of Pt/~~RuONO$_2$ sites on the electrode. This requires that relatively little nitrosyl complex be produced, which is the usual case. The isopotential point emphasizes the dominance of the k_3 pathway.

At very slow potential scan rates, the isopotential point appears between the Pt/~~RuNO$_2$ and Pt/~~RuONO$_2$ waves (Figure 2A) rather than the Pt/~~RuONO and Pt/~~RuONO$_2$ waves. This simply reflects the facile reversibility of the linkage isomerization reaction by which Pt/~~Ru^{III}ONO$_2$ can quantitatively reisomerize to Pt/~~Ru^{III}NO$_2$ at slow potential scan times.

Turning now to the relationship of Scheme I to the first-order rate result of Figure 3 and eq 3, we recognize the measured variable Γ_{RuNO_2} as $\Gamma_{Ru^{III}NO_2} + \Gamma_{Ru^{III}ONO}$ since at the slow potential scan rates used in the kinetic study the Pt/~~Ru^{III}NO$_2$ and Pt/~~Ru^{III}ONO states are freely interconvertible. Writing the rate law for the k_2 and k_3 reaction

Scheme II

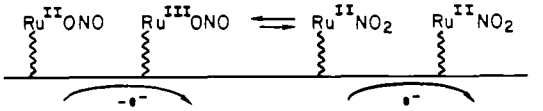

pathways in Scheme I and using a steady-state approximation for the Pt/~~Ru^{III}NO$_2$ state, we obtain

$$-d\Gamma_{RuNO_2}/dt = \frac{k_{-1}k_2[Pt/\sim\sim Ru^{III}ONO]^2}{k_1 + k_2[Pt/\sim\sim Ru^{III}ONO]} + k_3[Pt/\sim\sim Ru^{III}ONO] \quad (5)$$

Equation 5 shows that first-order behavior results if the k_3 term is large or if $k_1 \ll k_2$[Pt/~~Ru^{III}ONO]. The latter circumstance, in which k_{-1} becomes rate controlling, requires a much longer (ca. 200x) $t_{1/2}$ for the Pt/~~Ru^{III}ONO → Pt/~~Ru^{III}NO$_2$ conversion than the low-temperature voltammetry indicates is the case. The first-order rate results of Figure 3 thus most likely correspond to rate control by the k_3 pathway, which yields a predominance of Pt/~~RuONO$_2$ product in agreement with experiment.[14]

Finally, we should comment on the interesting situation of Figure 6. At low temperature, the Pt/~~Ru^{II}ONO linkage isomer, once formed by a rapid cathodic scan, is trapped and will persist for several minutes before reverting (k_4) to the nitro form. How then does an oxidative wave for Pt/~~Ru^{II}NO$_2$ nontheless always appear on an anodic scan of an electrode in the Pt/~~Ru^{II}ONO state and become relatively *larger* for a slow anodic scan? The formal potentials of the two isomers are such that electrode potentials applied at *intermediate* values will catalyze nitrito → nitro conversion at *zero net current flow*. This can be written for an anodic scan as Scheme II.

The above schemes satisfactorily account for all the voltammetry observed for the attached Pt/~~RuNO$_2$ complex. As noted above, Scheme I is qualitatively consistent with results obtained for $[(bpy)_2Ru(py)NO_2]^+$ in homogeneous solution. However, the advantages inherent in deriving the mechanism for the electrode-attached case should be reemphasized. When compared to conventional solution voltammetry, they include (1) the ease of carrying out low-temperature experiments, (2) the ability to use fast potential scans, (3) the experimental definition provided by symmetrical surface waves, and (4) the value of the isopotential point phenomenon.

Acknowledgment. This research was supported in part by grants from the National Science Foundation.

Registry No. II, 76318-60-0; $[(bpy)_2Ru(py)NO_2]^+$, 47735-73-9; enpt silane, 1760-24-3; $Ru(bpy)_2Cl_2$, 19542-80-4; Pt, 7440-06-4; PtO, 12035-82-4.

(13) See footnote 7 in ref 4. Further experiments on the outer-sphere oxidation of $[(bpy)_2Ru(py)NO_2]^+$ by $[(bpy)_3Ru]^{3+}$ in acetonitrile show that the ratios of nitrato to nitrosyl products are dependent on the ratio of $[(bpy)_3Ru]^{3+}$ to $[(bpy)_2Ru(py)NO_2]^+$ as follows ($[Ru(bpy)_3]^{3+}$/[$Ru(bpy)_2pyNO_2]^+$, NO_3/NO): 1/1, 1/1; 1.56/1, 3.2/1; 2.5/1, 6.8/1; 6/1, 22/1 (J. L. Walsh, Lafayette college, unpublished results, 1980).

(14) Recent results on the nitro complex immobilized by electroreductively initiated polymerization of $[(bpy)_2Ru(vinylpyridine)NO_2]^+$ are consistent with having the k_3 pathway as rate controlling. Experimental details and results will be given in a future publication.